Nitrate limitation and ocean acidification interact with UV-B to reduce photosynthetic performance in the diatom *Phaeodactylum tricornutum*

Running Title: Combined effects of NO_3^-, OA and UV

Wei Li[1,2], Kunshan Gao[1*], John Beardall[3]

[1] State Key Laboratory of Marine Environmental Science, Xiamen University (Xiang-An campus), Xiamen, Fujian, 361102 China

[2]College of Life and Environmental Sciences, Huangshan University, 245041, Huangshan, China

[3]School of Biological Sciences, Monash University, Clayton, VIC 3800, Australia

*Author for correspondence: ksgao@xmu.edu.cn (Kunshan Gao)

Abstract

It has been proposed that ocean acidification (OA) will interact with other environmental factors to influence the overall impact of global change on biological systems. Accordingly we investigated the influence of nitrogen limitation and OA on the physiology of diatoms by growing the diatom *Phaeodactylum tricornutum* Bohlin under elevated (1000 µatm, HC) or ambient (390 µatm, LC) levels of CO_2 with replete (110 µmol L^{-1}, HN) or reduced (10 µmol L^{-1}, LN) levels of NO_3^- and subjecting the cells to solar radiation with or without UV irradiance to determine their susceptibility to UV radiation (UVR, 280-400 nm). Our results indicate that OA and UVB induced significantly higher inhibition of both the photosynthetic rate and quantum yield under LN than under HN conditions. UVA or/and UVB increased the cells' non-photochemical quenching (NPQ) regardless of the CO_2 levels. Under LN and OA conditions, activity of superoxide dismutase and catalase activities were enhanced, along with the highest sensitivity to UVB and the lowest ratio of repair to damage of PSII. HC-grown cells showed a faster recovery rate of yield under HN but not under LN conditions. We conclude therefore that nutrient limitation makes cells more prone to the deleterious effects of UV radiation and that HC conditions (ocean acidification) exacerbate this effect. The finding that nitrate limitation and ocean acidification interact with UV-B to reduce photosynthetic performance of the diatom *P. tricornutum* implies that ocean primary production and the marine biological C pump will be affected by OA under multiple stressors.

Key words: CO_2, diatom, multiple stressors, nutrients, ocean acidification, photosynthesis, UV radiation

Abbreviations: DIC, dissolved inorganic carbon; NPQ, non-photochemical quenching; SOD, superoxide dismutase; CAT, catalase; Inh_{UVR}, inhibition due to UVR; *r*, repair rate; *k*, damage rate; CCMs, CO_2 concentrating mechanisms.

1 Introduction

Increasing atmospheric levels of CO_2 and the associated dissolution of CO_2 into the oceans has resulted in ocean acidification (OA), with increased levels of pCO_2, HCO_3^- and H^+ and decreased CO_3^{2-} concentration. The acidity of surface oceans has increased by 30% (lowered pH by 0.1 unit) since the Industrial Revolution and is expected to increase by 100-150% (0.3-0.4 pH units) by the year 2100 (Orr et al., 2005). At the same time, increased sea surface temperatures are predicted to cause a shoaling of the surface mixed layer, which in turn will lead to enhanced exposure to sunlight (both as photosynthetically active radiation (PAR) and as UVR). This enhanced stratification will also decrease upward transport of nutrients from deeper, nutrient rich layers, leading to more frequent/marked nutrient limitation (Cermeño et al., 2008). Global change is thus likely to cause changes in a multiplicity of factors that influence phytoplankton growth and it is thus critical to examine OA in the context of interactive effects with these other environmental drivers (Boyd, 2011).

Increased availability of CO_2 in seawater appears in some cases to bring a low level of benefit to growth and photosynthesis of natural phytoplankton populations

(Riebesell and Tortell, 2011) and references therein), though in most cases laboratory experiments have shown little effect of OA alone (Doney et al., 2009). However, the effects can differ according to changes in solar radiation and/or other physical or chemical factors (Gao et al., 2012a). Increased acidity of seawater may lead to physiological stress (Pörtner and Farrell, 2008) and affect phytoplankton nutrient uptake (Beman et al., 2011; Shi et al., 2012). Therefore, OA could most likely result in differential effects on different photosynthetic organisms or under different environmental conditions (Gao, 2011).

Diatoms account for about 20% of the total global primary production and about 40% of that in the oceans (Granum et al., 2005). Early reports suggested that growth of diatom species could be limited by the availability of CO_2 (Riebesell et al., 1993). However, the growth rate of diatom-dominated natural phytoplankton populations was not affected by CO_2 enrichment to 800 μatm (Tortell, 2000), and not all diatom species were sensitive to seawater pCO_2 rise under nutrient-replete conditions in a mesocosm study (Kim et al., 2006). In laboratory experiments, growth of *Skeletonema costatum* was not stimulated by elevated CO_2 (800 μatm) (Chen and Gao, 2011). *Phaeodactylum tricornutum* grown under nitrate-limited conditions also showed no enhancement of growth under high CO_2 (1000 μatm) (Li et al., 2012a). Nevertheless, in other work, the diatoms *Phaeodactylum tricornutum* (1000 μatm) (Wu et al., 2010) and *Attheya* sp. (670 μatm) (King et al., 2011) showed enhanced growth rate in nutrient replete conditions under elevated CO_2 levels. These variable findings reflect physiologically differential

responses among different species or under different experimental or environmental conditions. Changes in light intensity can lead to enhanced, unaffected or inhibited growth rates under OA conditions, even for the same diatom species (Gao et al., 2012b). Recently, microcosm studies have shown that the species abundance and physiological responses (eg. Chl *a*, DNA damage, ROS, photosynthetic efficiency) could be regulated by nutrients and light availability under high CO_2 conditions (Neale et al., 2014; Sobrino et al., 2014). Therefore, the effects of OA should be considered in the context of the influence of multiple factors, such as temperature, nutrient status, light and UVR (Boyd, 2011; IPCC, 2011; Gao et al., 2012a).

Solar UVB radiation (280-315 nm), which is increasing due to interactions of global change and ozone depletion (Häder et al., 2011), is known to damage DNA (Buma et al., 2003; Gao et al., 2008), lower photosynthetic rates (Helbling et al., 2003), perturb the uptake of nutrients (Hessen et al., 2008) and alter morphological development (Wu et al., 2005) of phytoplankton. In contrast, under moderate levels of solar radiation, solar UVA radiation (315-400 nm) is known to stimulate photosynthesis (Gao et al., 2007), signaling (Cashmore, 1998) and photo-repair of UVB-induced damage (Buma et al., 2003) in phytoplankton. Previously, it was shown that UV-induced inhibition of dinoflagellates was lower under nutrient replete conditions but higher under nutrient limitation, due to less efficient repair resulting from lowered nutrient availability (Litchman et al., 2002). Similar enhancement of UVB impacts under nutrient (N, P) limitation were shown for a green microalga, *Dunaliaella tertiolecta* (Shelly et al., 2002; Heraud et al., 2005). Recently, OA was

found to enhance UVB-induced damage to a red tide alga, *Phaeocystis globosa*, leading to a greater decrease in growth rate and photochemical yield under 1000 μatm CO_2 (Chen and Gao, 2011).

Marine phytoplankton often experience nutrient limitation in offshore waters; with progressive ocean warming, such limitation will be intensified due to decreased depth of the surface mixed layer (enhanced stratification) (Cermeño et al., 2008). Combined effects of nutrient levels and CO_2 have been reported in many studies. For example, photosynthetic carbon fixation of the coccolithophorid *Emiliania huxleyi* was enhanced under high light and low nitrogen conditions when the seawater CO_2 concentration was raised to 2000 μatm (Leonardos and Geider, 2005). However, increased seawater CO_2 concentration also showed antagonistic effects with iron in modulating (down- or up-regulating) primary production of marine phytoplankton in the Gulf of Alaska (a nutrient replete but low chlorophyll area) (Hopkinson et al., 2010). In some toxin producing species, for example the dinoflagellate *Karlodinium veneficum*, toxicity was enhanced under high CO_2 and low phosphate conditions (Fu et al., 2010). However, to the best of our knowledge, there is little information concerning the combined effects of OA and NO_3^- limitation on diatoms and their susceptibility to damage from solar UVR (280-400 nm).

Nutrient availability can influence phytoplankton responses to UV and to CO_2-induced seawater acidification. Theoretically, increased seawater acidity can perturb intracellular acid-base balance and thus lead to differential interactions between nutrients and solar UVR. In this study, we hypothesize that reduced

133 availability of NO_3^- under OA would affect the photosynthetic performance under
134 solar radiation with or without UVR. We used the diatom *Phaeodactylum tricornutum*
135 to test this hypothesis.
136
137 **2 Materials and methods**
138 **2.1 Growth conditions**
139 The diatom *Phaeodactylum tricornutum* Bohlin (strain CCMA 106), isolated
140 from the South China Sea (SCS) and maintained in the Center for Collections of
141 Marine Bacteria and Phytoplankton (CCMBP) of the State Key Laboratory of Marine
142 Environmental Sciences (Xiamen University), was grown mono-specifically in
143 artificial seawater enriched with Aquil medium (Morel et al., 1979). Cells were
144 cultured in 500 mL vessels containing 250 mL medium under two levels of NO_3^- (110
145 μmol L^{-1}, HN; 10 μmol L^{-1}, LN) and aerated with ambient (outdoor) air (LC, 390
146 μatm) or elevated (1000 μatm, HC) CO_2 levels within a plant CO_2 chamber
147 (HP1000G-D, Ruihua instrument & equipment Co. Ltd, China). Gas flow rate was
148 300 ml min^{-1}, and the CO_2 concentrations varied by less than 3% of the target value.
149 The low NO_3^- level of 10 μmol L^{-1} was based on its concentration range (ca. 0-20
150 μmol L^{-1}) in the oligotrophic SCS, from where the diatom strain was isolated.
151 Dilutions were made every 24 h, so that the seawater carbonate system was
152 maintained stable under each CO_2 level within the cell density range of 6×10^4 to $3 \times$
153 10^5 cells ml^{-1} (exponential growth phase). According to the pre-experiment, the initial
154 nitrate concentration of 10 μmol L^{-1} could be totally consumed (0-10 μmol L^{-1}) ; and the

initial nitrate concentration of 110 μmol L^{-1} treatment, the nitrate ranged from ca. 85-110 μmol L^{-1} during the culture. The cells were grown at 70 μmol photons m^{-2} s^{-1} (cool white fluorescent tubes) under a 12L: 12D photoperiod for at least 10 generations before being used for the solar radiation treatments described below. Three independent cultures were grown at each condition.

2.2 Determination of seawater carbonate system parameters

The pH in the cultures was determined daily during the light period with a pH potentiometric titrator (DL15, Mettler-Toledo, Schwerzenbach, Switzerland), which was calibrated with NBS (National Bureau of Standards) buffer solutions (Hanna). DIC (dissolved inorganic carbon) was estimated with an automatic system (AS-C3, Apollo Scitech) linked to an infrared gas detector (Li-Cor 7000, Li-Cor). DIC, pH, nutrient concentrations (phosphate, 10 μmol L^{-1}; silicate, 100 μmol L^{-1}), salinity (35) and temperature (20°C) were used to calculate the parameters of the seawater carbonate system (HCO_3^-, CO_3^{2-}, CO_2 and TA) using the CO_2 system analyzing software CO_2SYS (Lewis and Wallace, 1998) as described previously (Li et al., 2012a). The carbonic acid dissociation constants (K_1 and K_2) used were those of Roy et al. (1993), and that for boric acid (K_B) was from Dickson (1990).

2.3 Radiation treatments under the solar simulator

To determine the effects of growth conditions on the sensitivity of carbon fixation and chlorophyll fluorescence to short-term exposure to UVR, *P. tricornutum* cells,

177 grown under LC-LN (low CO_2 + low nitrate), HC-LN (high CO_2 + low nitrate),
178 LC-HN (low CO_2 + high nitrate) and HC-HN (high CO_2 + high nitrate) conditions,
179 were exposed for 1 h to different radiation treatments with or without UVR, as
180 follows: 1) P treatment, tubes wrapped with Ultraphan film 395 (UV Opak, Digefra),
181 being exposed to PAR alone; 2) PA treatment, tubes wrapped with Folex 320
182 (Montagefolie, Folex, Dreieich, Germany), receiving wavelengths above 320 nm
183 (PAR+UVA); 3) PAB treatment, tubes wrapped with Ultraphan Film 295 (Digefra,
184 Munich, Germany), so that the cells received wavelengths above 295 nm
185 (PAR+UVA+UVB). The transmission spectra of the cut-off filters are available
186 elsewhere (Zheng and Gao, 2009). Samples were placed at a distance of 1.2 m from a
187 solar simulator (Sol 1200W, Dr. Hönle, Martinsried, Germany), so that the actual PAR
188 light intensities to which the cells were exposed within the tubes (calculated taking
189 into account the transmission properties of the quartz tubes and the filters) was 44.11
190 Wm^{-2} (ca. 190.11 μmol photons m^{-2} s^{-1}) which is close to the daytime mean photon
191 flux in the middle of the photic zone (22-36 m depth in South China Sea, SEATS
192 station). The corresponding UVA and UVB irradiances were 14.19 Wm^{-2} (ca. 41.99
193 μmol photons m^{-2} s^{-1}) and 0.75 Wm^{-2} (ca. 1.89 μmol photons m^{-2} s^{-1}). Irradiances
194 were measured with a broad-band filter radiometer (ELDONET, Real Time Computer,
195 Möhrendorf, Germany). After the radiation treatments, the cells were replaced under
196 their growth light level (70 μmol photons m^{-2} s^{-1}) to examine the recovery of
197 photosynthetic performance. During the incubations, the tubes were maintained in a
198 water bath at 20 ℃ using a circulating cooler (Eyela, CAP-3000, Tokyorikakikai Co.

199 Ltd., Tokyo, Japan).

200

201 **2.4 Measurement of carbon fixation**

202 The ^{14}C method was applied to measurements of marine photosynthetic carbon
203 fixation (Nielsen, 1952), and has been detailed with modified protocols in many
204 publications (Holm-Hansen and Helbling, 1995; Gao et al., 2007). Cells were
205 harvested in the middle of the light phase, diluted with freshly made medium
206 equilibrated with the designated concentrations of CO_2 to a cell concentration of 2-3 ×
207 10^4 cells ml^{-1} and transferred to 35 ml quartz tubes. Each tube was injected with 100
208 μl-5 μCi (0.185 MBq) $NaH^{14}CO_3$ solution (ICN Radiochemicals). Triplicate
209 incubations were carried out for each treatment as mentioned above and, additionally,
210 3 tubes were wrapped in aluminum foil and incubated as a dark control. The cells
211 were collected on Whatman GF/F glass filters either immediately after 1 h exposure
212 to the solar simulator or after a period of recovery under their growth light for another
213 hr. The filters were put into 20 ml scintillation vials, fumed with HCl for 12 h and
214 then dried for 6 h at 45 ℃ to expel the non-fixed inorganic carbon as CO_2.
215 Scintillation cocktail (3 mL of Tri-Carb 2800TR, Perkin Elmer®) was added to the
216 vials, and radioactivity in the vials counted with a liquid scintillation counter (LS
217 6500, Beckman Coulter, USA). Carbon fixation rates were calculated from these
218 counts and are presented on a per cell basis or per chl *a*.

219

220 **2.5 Measurement of Chlorophyll fluorescence**

For chlorophyll fluorescence measurements, cell collection and radiation treatments were carried out as described above. The effective quantum yield (yield) was measured every 20 min either during the solar simulator exposure or during recovery under the growth light level.

The effective quantum yield (yield) and non-photochemical quenching (NPQ) parameters were calculated according to Genty et al. (1990) as yield = $(F'_m - F_t) / F'_m$ and NPQ = $(F_m - F'_m) / F'_m$, respectively, where F_m is the maximum fluorescence yield after 15 min dark adaptation, F'_m is the light-adapted maximal chlorophyll fluorescence yield measured during the exposures, and F_t is the steady fluorescence level during the exposures. The actinic light was set at the growth light level, and the saturating pulse (5000 μmol photons m^{-2} s^{-1}) lasted for 0.8 s.

Repair (r) and damage (k) rates during the 60 min exposure period in the presence of UV were calculated using the Kok model (Heraud and Beardall, 2000): $P/P_{initial} = r/(k+r)+[k/(k+r)]e^{-(k+r)t}$, where $P_{initial}$ and P were the yield values at beginning and at exposure time t.

During the recovery period, the exponential rate constant for recovery (R) was calculated from the following equation: $y = y_o+b\times[1-\exp(-R\times t)]$, where y represents the yield value at time t, y_o is the starting value before recovery and b is a constant.

The relative inhibitions of carbon fixation or yield caused by UVA or UVB were calculated as follows:

$Inh_{UVR} = (P_{PAR} - P_{PAB}) / P_{PAR} \times 100\%$;

$Inh_{UVA} = (P_{PAR} - P_{PA}) / P_{PAR} \times 100\%$;

243 $Inh_{UVB} = Inh_{UVR} - Inh_{UVA}$;

244 where P_{PAR}, P_{PA} and P_{PAB} represent carbon fixation or yield values under PAR,
245 PAR + UVA, PAR + UVA + UVB treatments, respectively.

246

247 **2.6 Cells counts and chlorophyll *a* measurements**

248 The cells were counted using a Z2^{TM} Coulter Counter (Beckman, USA). Where
249 needed, we used the values for chlorophyll *a* (chl *a*) contents of the cells grown under
250 the same CO_2 and nitrate levels reported previously (Li et al., 2012a).

251

252 **2.7 Total protein content, superoxide dismutase (SOD) and catalase (CAT)**
253 **measurements**

254 To determine the total protein content and activities of SOD and CAT, cells were
255 collected, in the middle of the light phase, onto a polycarbonate membrane (0.22 μm,
256 Whatman) under vacuum at a pressure of less than 0.1 Pa and washed into a 1 ml
257 centrifuge tube with phosphate buffer (pH 7.6). The enzyme extractions were carried
258 out in 0.6 ml phosphate buffer (pH 7.6) that contained 50 mM KH_2PO_4, 1 mM
259 Ethylene Diamine Tetraacetic Acid (EDTA), 0.1% Triton X-100 and 1% (w/v)
260 polyvinyl polypyrrolidone. The cells were broken by sonication in an ice-water bath
261 (4 ℃), and the homogenized extract was centrifuged at 12000 g (4 ℃) for 10 min
262 before the activities of SOD and CAT were tested with SOD and CAT Assay Kits
263 (Nanjing Jiancheng Biological Engineering Company, China). One unit of SOD was
264 defined as the amount causing a 50% inhibition of nitroblue tetrazolium (NBT)

reduction (Wang and Wang, 2010). One unit of CAT activity was defined as the amount required to decompose 1 μmol H_2O_2 per second. The SOD and CAT activities were expressed as U mg^{-1} protein and per 10^6 cells (Fig. S1). The total protein content was determined according to Bradford (1976) using bovine serum albumin as the standard.

2.8 Statistical analyses and calculations

One-way analysis of variance (ANOVA) was used, followed by a multiple comparison using a Tukey-test to establish differences among the treatments. Interactive effects among CO_2, NO_3^- and UVR on carbon fixation and yield were determined using a two- or three-way ANOVA to establish significant differences among the variables.

3 Results

3.1 Carbon fixation

Carbon fixation was significantly inhibited by UVR in both HN and LN-grown cells either based on per cell or chl *a* (Fig.1). Under the HN conditions, the carbon fixation rates of LC and HC cultures, compared to that of PAR alone treatment, were inhibited by 29.4% ($P = 0.0002$) and 36.7% ($P < 0.0001$) in the presence of UVA (PA treatment: PAR+UVA), and by 47.7% ($P < 0.0001$) and 46.1% ($P = 0.0029$) with both UVA and UVB (PAB, PAR+UVA+B) (Fig. 1a and c). However, the carbon fixation per cell in the LC grown cells was 10.0% ($P = 0.0058$) higher in those exposed to PA,

287 and that based on chl *a* was higher under the PAR alone or PA treatments, by about
288 8.4% (P = 0.0253) and 17.9% (P = 0.005) compared to that of the HC-grown cells.
289 For PAB treatments, there were no significant differences between the HC and
290 LC-grown cells (Fig. 1a and c).

291 Under LN conditions, carbon fixation rates of LC and HC grown cells were
292 decreased by 14.7 % (P = 0.0039) and 1.1% (P = 0.8658) in the presence of UVA (PA)
293 and by 23.3% (P = 0.0019) and 27.3% (P = 0.0123) with UVA and UVB (PAB)
294 treatments, respectively (Fig. 1b and d), compared with that of PAR alone treatment.
295 That is, both UVA and UVB resulted in significant impacts in the LN-grown cells
296 under LC, but only UVB brought about significant reduction of the rate under HC. In
297 the PA treatment, the HC-LN cells fixed carbon at a rate 21.7% (P = 0.0071) higher
298 than in the LC-LN cells (Fig. 1b), however, there were no significant differences
299 between HC and LC cells in the PAR and the PAB treatments under N-limitation.
300 Under the LN level, the carbon fixation rate per chl *a* was about 30.8% (P = 0.01),
301 51.6% (P = 0.0013) and 24.0% (P = 0.03) higher in HC than in LC-grown cells (Fig.
302 1d).

303

304 **3.2 Photochemical quantum yield**

305 When exposed to different irradiation treatments, photochemical quantum yields
306 ('yield') in the cells grown under either HC or LN conditions showed similar patterns
307 with those grown at LC and HN conditions (Fig. 2), decreasing rapidly during the
308 initial 20 min and leveling off after 40 to 60 min. Under HN conditions, the yield in

309 the HC-grown cells decreased to a similar level among the treatments (P, P = 0.1568;
310 PA, P = 0.0879; PAB, P = 0.1341) as that in the LC-treatments (Fig. 2a and b). Under
311 the LN condition, the yield decreased to much lower levels compared to those under
312 HN treatments (Fig. 2c and d). Cells exposed to all treatments showed recovery of the
313 yield, under their growth light (70 μmol photons m^{-2} s^{-1}), to approximately their initial
314 levels in about 80 min (Fig 3).
315
316 **3.3 UVA and UVB induced inhibition of photosynthetic performance**
317 While UVA induced significantly higher (P = 0.0114) inhibition of photosynthetic
318 carbon fixation in the HC-HN but lower (P = 0.0038) in the HC-LN grown cells (Fig.
319 3a and b), it did not cause significant changes in the yield between the HC- and LC-
320 grown cells (HN, P = 0.1375; LN, P = 0.0500) (Fig. 3c). While the contribution of
321 UVB did not induce significant inhibition of either carbon fixation (P = 0.2308) or
322 yield (P = 0.5319) in the HN-grown cells, under both the HC and LC conditions (Fig.
323 3a and c), it caused significantly higher inhibition of the photosynthetic rate (by
324 203.3%, P = 0.0006) and the yield (by 76.8%, P = 0.0451) in the HC- than the LC-
325 grown cells under NO_3^- limited conditions (Fig. 3b and d). Interactive effects among
326 CO_2, NO_3^- and radiation treatments on yield were significant (Table 1).
327
328 **3.4 Repair, damage rates and constant for recovery rate**
329 The HC-grown cells had higher rates of damage, k, than the LC-grown cells
330 under nitrogen limitation but not under N replete conditions (HN, P = 0.2109; LN, P

331 = 0.0092). No effect was observed for repair rates *r* (HN, *P* = 0.1655; LN, *P* =
332 0.5276). The repair:damage (r/k) ratios in the HC-grown cells showed a 21.0% (but
333 statistically insignificant) increase under HN (*P* = 0.3450) but decreased significantly
334 by 31.1% under LN (*P* = 0.0320) conditions, compared to the LC-grown cells,
335 respectively (Table 2). Under the low PAR, the exponential rate constant for recovery
336 (R) showed dependency on previous light treatments with lowered rate in the cells
337 exposed to UVR, while HC stimulated the rate under the HN but not LN condition
338 (Table 3). Obviously, the cells exposed to the radiation treatments with UVB took
339 longer ($P < 0.05$) to recover their photochemical yield, and pre-exposure to UVA had
340 little ($P > 0.05$) effect on the recovery; HC-HN-grown cells had faster ($P < 0.05$)
341 photochemical recovery (Table 4).
342
343 **3.5 Non-photochemical quenching (NPQ)**
344 Non-photochemical quenching (NPQ) showed an opposite pattern of change to
345 yield during both the exposure and recovery periods (Fig. 4). Under HN conditions,
346 HC treatments triggered the highest NPQ within 20 min (Fig. 4a), while NPQ reached
347 its maximal values at 40 min under the ambient (LC) CO_2 level (Fig. 4b). Similar
348 trends were found in both the LN and HN grown cells regardless of the radiation
349 treatments (Fig. 4). Both UVA and UVB caused additional ($P < 0.05$) rises in NPQ in
350 HN-grown cells regardless of the CO_2 levels (Fig. 4a and b). However, neither UVA
351 nor UVB induced significant ($P > 0.05$) change in NPQ in LN-grown cells, regardless
352 of the CO_2 levels (Fig. 4c and d). Lower NPQ values were found in HN-grown cells

353 compared with LN, under either PAR alone or PAR+UVA treatments. Addition of
354 UVB, however, resulted in an approximately 17.0% higher, but statistically
355 insignificant (LC, P = 0.1150; HC, P = 0.1660), increase of NPQ in HN compared to
356 LN-grown cells. Transfer to the growth light level without UV, to allow recovery, led
357 to a rapid decline of NPQ with time. For the cells that were pre-exposed to the
358 PAR+UVA+B treatment, relaxation of NPQ during the recovery period showed no
359 difference (P > 0.05) between HC- and LC-grown cells except that NPQ in the
360 HC-HN grown cells declined faster (P = 0.0242) than in LC-HN cells. Two-way
361 ANOVA showed that both nitrogen levels and radiation treatments individually, and
362 also interactively, affected the NPQ (Table 1).
363
364 **3.6 Protein content, SOD and CAT activities**
365 Protein contents were enhanced in HN cultures under both LC (3.21 ±0.98 pg
366 $cell^{-1}$) and HC (3.38 ±1.35 pg $cell^{-1}$) conditions, compared with LN grown cells (LC,
367 2.58 ±0.46 pg $cell^{-1}$; HC, 2.28 ±0.68 pg $cell^{-1}$), though statistically there were no
368 significant differences among the treatments (P = 0.4296) (Fig. 5a). There was no
369 significant difference in protein content between LC and HC treatments at a given
370 NO_3^- concentration. However, NO_3^--limitation enhanced SOD (LC, by 62.5%, P =
371 0.0004; HC, by 72.5%, P = 0.0007) and CAT (LC, by 67.5%, P = 0.0759; HC, by
372 67.1%, P = 0.0747) activities in both LC and HC-grown cells, when based on protein
373 content (Fig. 5b and c), though such enhancement was insignificant (P > 0.1) when
374 normalized to per cell (Fig. S1).

4 Discussion

This study shows that nitrate limitation interacts with OA to affect the overall impacts of solar UVR on the diatom *P. tricornutum*. OA and UVB caused significantly higher inhibition of the photosynthetic rate and the quantum yield under LN than under HN conditions. Interactive effects of reduced nitrate availability and OA increased protein-based activity of superoxide dismutase (SOD) and catalase (CAT) but decreased the rate of repair of PSII from UV-induced damage. OA appeared to counteract UVB-induced damage under NO_3^- replete conditions, but when combined with decreased availability of nitrate, it increased the diatom's sensitivity to UVR.

Most diatoms have evolved CO_2 concentrating mechanisms (CCMs) as a response to low availability of CO_2 in the present-day oceans (Raven et al., 2011). Increasing pCO_2 may, to some extent, benefit marine phytoplankton due to increased availability of CO_2 (Burkhardt et al., 2001; Rost et al., 2003). CCMs are known to be down-regulated under a CO_2 level doubling that of the current ambient concentration, saving about 20% of the energy cost for active inorganic carbon acquisition in some diatoms (including *P. tricornutum*) (Hopkinson et al., 2011). Such a down-regulation of CCMs was equally obvious in *P. tricornutum* grown under nitrate-limited or replete conditions (Wu et al., 2010; Li et al., 2012a). However, this down-regulated CCM and its effects may be mediated by many other factors. A recent study found that different acclimation times (short term, 15-16 generations and longer term, 33-57 generations)

to increased CO_2 and nitrate limitation may have different effects on the DIC and DIN uptake rate in diatom *Thalassiosira pseudonana*, with short-term acclimated cells showing a linear correlation with changes in fCO_2 although this was not the case in long-term acclimated cells (Hennon et al., 2014). On the other hand, the down-regulation of CCM operation was recently shown to decrease the growth of 3 diatoms (*Phaeodactylum tricornutum, Thalassiosira pseudonana* and *Skeletonema costatum*) under high levels of sunlight but to enhance it under low light (Gao et al., 2012b). The growth rate of *P. tricornutum* under high CO_2 (1000 μatm) decreased at light levels higher than 180 μmol m^{-2} s^{-1} to be lower than that of the low CO_2-grown cells (Gao et al., 2012b). In the present study, under the near-saturation light level (ca. 190 μmol photons m^{-2} s^{-1} of PAR), photosynthetic carbon fixation rate per chl *a* under the nitrate limited condition was higher in the HC-grown cells. Obviously, the nutrient limitation influenced the effects of OA.

UVR is known to damage photosynthetic pigments and proteins (for example D1 and Rubisco proteins) (Zacher et al., 2007) and therefore would reduce the photosynthetic capacity of algae (Häder et al., 2011). UVA induced significantly higher inhibition of carbon fixation in HC-HN than in LC-HN grown cells, reflecting a synergistic effect of UVA and OA; however, for the same cells, UVB induced no greater inhibition of the photosynthetic carbon fixation in HC compared to LC cells, which is in contrast to the findings reported in another study (Li et al., 2012b). Many studies have shown that the sensitivity of cells to high levels of PAR and UV under OA condition could be stimulated and then induce higher inhibition rate of

419 photosynthesis (Sobrino et al., 2008; Gao et al., 2012b; Xu and Gao, 2012). However,
420 this phenomenon is not always found in all species especially when the intensity of
421 PAR or UV is not that high. For example, a recent study reported that the unicellular
422 chlorophyte (*Dunaliella tertiolecta*) acclimated with high CO_2 under nutrient replete
423 conditions could alleviate the stress induced by high PAR and UV (García-Gómez et
424 al., 2014). This could be due to the energy saving as a result of down-regulation of CCM
425 activity. However, in the present study, we did not find that the synergistic effects of OA
426 and UVR induced a higher inhibition at the light intensity of PAR+ UVA+UVB (44.11 +
427 14.19 + 0.75 Wm^{-2}) used, than found under LC. This may be due to the light intensity of
428 PAR or UVR not being high enough to exceed the energy dissipating capacity of the cells.
429 Furthermore, under high N the nutrient supply would be sufficient to support the repair
430 processes of UV or high PAR induced damage. In the LN-grown cells, UVB induced
431 greater inhibition of both carbon fixation and yield, probably due to a decreased
432 repair/damage ratio (Table 2) and decreased levels of both chl *a* and other light
433 harvesting pigments (Li et al., 2012a), since the (re)synthesis of both proteins and
434 UV-screening compounds depends on nitrogen availability (Beardall et al., 2009;
435 Beardall et al., 2014). Such an inhibition by UVB in LN-grown cells was more
436 pronounced under OA conditions (Fig. 3b and d), though UVB appeared to counteract
437 the OA effect under the HN condition. When the cells are exposed to lower external
438 pH, they would need additional energy to cope with the acid-base perturbation
439 (Kanazawa and Kramer, 2002). By impairing photosynthesis, nitrogen limitation
440 could decrease the supply of energy, especially in the presence of UVB (Döhler,

441 1998). Though SOD and CAT normalized per cell showed no change in all treatments
442 (Fig. S1), the fact that nitrogen limitation led to decreased protein contents per cell
443 and with higher activity of SOD and CAT (based on protein content) implies that
444 these enzymes are preferentially retained in the face of decreasing protein per cell and
445 thus reflects an enhanced defense strategy (Fig. 5), so that reactive oxygen species
446 (ROS) that were formed under N-limitation could be scavenged. The differential
447 impacts of UVB on HN and LN-grown cells under the OA treatment could be due to
448 differences in the repair and damage rates (Table 2) and differential stimulation of
449 periplasmic proteins (Wu and Gao, 2009), which are important transporters of ions
450 and play important roles in maintaining intracellular acid-base stability. On the other
451 hand, NO_3^- scarcity usually leads to an impaired PSII reaction center activity due to
452 decreased synthesis of key proteins, therefore, leading to decreased quantum yields of
453 PSII (Geider et al., 1993). In this study, *P. tricornutum* showed much lower yield (Fig.
454 2c and d), as well as NPQ, in the nitrogen limited cells (Fig. 4c and d), indicating
455 smaller functional PSII reaction centers and a lower heat dissipating capability, when
456 combined with the OA treatment, consistent with these cells having the highest
457 damage and the lowest repair (Table 2). In the HN-grown cells, better recovery of
458 both photosynthetic carbon fixation (data not shown) and photochemical performance
459 (Table 3, 4) under the OA condition could be attributed to faster repair rate of PSII
460 and related metabolic up-regulations.

461 The results from the present work suggest that nutrient limitation can alter the
462 effects of OA or UVR and their interactions. In the oligotrophic oceans, such as the

surface mixed layers of the South China Sea (SCS), where averaged total inorganic nitrogen concentrations range from 0-20 μmol, UVB and OA can act synergistically to bring about a higher inhibition of photosynthetic carbon fixation. Higher UVB-induced inhibition of photosynthesis was found in pelagic low-nutrient waters than in coastal waters in the SCS (Li et al., 2011). With enhanced stratification and reduced thickness of the upper mixed layer due to ocean warming, fewer nutrients will be transported from deeper layers to the photic zones, and interactions of enhanced nutrient limitation, OA and increased solar exposures will become the main drivers influencing marine primary production (Gao et al., 2012a). For the diatoms, such as *P. tricornutum*, OA and other ocean changes may result in transitions in their vertical and horizontal distributions and changes in phytoplankton community structure.

Author contribution

K.G. and W.L. conceived and designed the experiments, W.L. performed the experiments. W.L., K.G. and J.B. analyzed the data and wrote the paper.

Acknowledgements

This study was supported by National Natural Science Foundation (41120164007, 41430967), by Joint project of NSFC and Shandong province (Grant No. U1406403), Strategic Priority Research Program of CAS (Grant No. XDA11020302), Program for Chang-jiang Scholars and Innovative Research Team (IRT_13R51), SOA

485 (GASI-03-01-02-04) and China-Japan collaboration project from MOST
486 (S2012GR0290). JB's work on climate change effects on algae has been funded by
487 the Australian Research Council and his visit to Xiamen was supported by '111'
488 project from Ministry of Education. We thank Yahe Li (Xiamen University, China) for
489 her kind assistance during the experiments.
490

491 **References**

492 Beardall, J., Sobrino, C., and Stojkovic, S.: Interactions between the impacts of
493 ultraviolet radiation, elevated CO_2, and nutrient limitation on marine primary
494 producers, Photochem. Photobio. S., 8, 1257-1265, 2009.
495 Beardall, J., Stojkovic, S., and Gao, K.: Interactive effects of nutrient supply and other
496 environmental factors on the sensitivity of marine primary producers to
497 ultraviolet radiation: implications for the impacts of global change, Aquat. Biol.,
498 22, 5-23, 2014.
499 Beman, J. M., Chow, C.-E., King, A. L., Feng, Y., Fuhrman, J. A., Andersson, A.,
500 Bates, N. R., Popp, B. N., and Hutchins, D. A.: Global declines in oceanic
501 nitrification rates as a consequence of ocean acidification, Proc. Natl. Acad. Sci.
502 U. S. A., 108, 208-213, 2011.
503 Boyd, P. W.: Beyond ocean acidification, Nat. Geosci., 4, 273-274, 2011.
504 Bradford, M. M.: A rapid and sensitive method for the quantitation of microgram
505 quantities of protein utilizing the principle of protein-dye binding, Anal.
506 Biochem., 72, 248-254, 1976.
507 Buma, A. G. J., Boelen, P., and Jeffrey, W. H.: UVR-induced DNA damage in aquatic

organisms. In: UV effects in aquatic organisms and ecosystems, Helbling, E. W. and Zagarese, H. E. (Eds.), The Royal Society of Chemistry, Cambridge, UK, 291-327, 2003.

Burkhardt, S., Amoroso, G., Riebesell, U., and Sültemeyer, D.: CO_2 and HCO_3^- uptake in marine diatoms acclimated to different CO_2 concentrations, Limnol. Oceanogr., 46, 1378-1391, 2001.

Cashmore, A. R.: The cryptochrome family of blue/UV-A photoreceptors, J. Plankton Res., 111, 267-270, 1998.

Cermeño, P., Dutkiewicz, S., Harris, R. P., Follows, M., Schofield, O., and Falkowski, P. G.: The role of nutricline depth in regulating the ocean carbon cycle, Proc. Natl. Acad. Sci. U. S. A., 105, 20344-20349, 2008.

Chen, S. and Gao, K.: Solar ultraviolet radiation and CO_2-induced ocean acidification interacts to influence the photosynthetic performance of the red tide alga *Phaeocystis globosa* (Prymnesiophyceae), Hydrobiologia, 675, 105-117, 2011.

Döhler, G.: Effect of ultraviolet radiation on pigmentation and nitrogen metabolism of Antarctic phytoplankton and ice algae, J. Plant Physiol., 153, 603-609, 1998.

Dickson, A. G.: Standard potential of the reaction: AgCl(s) + ½ H_2(g) = Ag(s) + HCl(aq), and the standard acidity constant of the ion HSO_4^- in synthetic seawater from 273.15 to 318.15 K, J. Chem. Thermodyn., 22, 113-127, 1990.

Doney, S. C., Fabry, V. J., Feely, R. A., and Kleypas, J. A.: Ocean acidification: The other CO_2 problem, Annu. Rev. Mar. Sci., 1, 169-192, 2009.

Fu, F., Place, A. R., Garcia, N. S., and Hutchins, D. A.: CO_2 and phosphate

availability control the toxicity of the harmful bloom dinoflagellate *Karlodinium veneficum*, Aquat. Microb. Ecol., 59, 55-65, 2010.

Gao, K.: Positive and negative effects of ocean acidification: Physiological responses of algae, Journal of Xiamen University (Natural Science), 50, 411-417, 2011.

Gao, K., Helbling, E. W., Häder, D. P., and Hutchins, D. A.: Responses of marine primary producers to interactions between ocean acidification, solar radiation, and warming, Mar. Ecol. Prog. Ser., 470, 167-189, 2012a.

Gao, K., Li, P., Watanabe, T., and Helbling, E. W.: Combined effects of ultraviolet radiation and temperature on morphology, photosynthesis, and DNA of *Arthrospira (Spirulina) platensis* (Cynophyta), J. Phycol., 44, 777-786, 2008.

Gao, K., Wu, Y., Li, G., Wu, H., Villafañe, V. E., and Helbling, E. W.: Solar UV radiation drives CO_2 fixation in marine phytoplankton: a double-edged sword, Plant Physiol., 144, 54-59, 2007.

Gao, K., Xu, J., Gao, G., Li, Y., Hutchins, D. A., Huang, B., Wang, L., Zheng, Y., Jin, P., Cai, X., Häder, D. P., Li, W., Xu, K., Liu, N., and Riebesell, U.: Rising CO_2 and increased light exposure synergistically reduce marine primary productivity, Nat. Clim. Change., 2, 519-523, 2012b.

García-Gómez, C., Gordillo, F. J., Palma, A., Lorenzo, M. R., and Segovia, M.: Elevated CO_2 alleviates high PAR and UV stress in the unicellular chlorophyte *Dunaliella tertiolecta*, Photochem. Photobio. S., 13, 1347-1358, 2014.

Geider, R. J., Roche, J., Greene, R. M., and Olaizola, M.: Response of the photosynthetic apparatus of *Phaeodactylum tricornutum* (Bacillariophyceae) to

552 nitrate, phosphate, or iron starvation, J. Phycol., 29, 755-766, 1993.
553 Genty, B., Harbinson, J., and Baker, N. R.: Relative quantum efficiencies of the
554 two-photosystems of leaves in photorespiratory and non-photorespiratory
555 conditions, Plant Physiol. Bioch., 28, 1-10, 1990.
556 Granum, E., Raven, J. A., and Leegood, R. C.: How do marine diatoms fix 10 billion
557 tonnes of inorganic carbon per year?, Can. J. Bot., 83, 898-908, 2005.
558 Häder, D.-P., Helbling, E. W., Williamson, C. E., and Worrest, R. C.: Effects of UV
559 radiation on aquatic ecosystems and interactions with climate change,
560 Photochem. Photobio. S., 10, 242-260, 2011.
561 Helbling, E. W., Gao, K., Gonçalves, R. J., Wu, H., and Villafañe, V. E.: Utilization of
562 solar UV radiation by coastal phytoplankton assemblages off SE China when
563 exposed to fast mixing, Mar. Ecol. Prog. Ser., 259, 59-66, 2003.
564 Hennon, G. M. M., Quay, P., Morales, R. L., Swanson, L. M., and Virginia Armbrust,
565 E.: Acclimation conditions modify physiological response of the diatom
566 *Thalassiosira pseudonana* to elevated CO_2 concentrations in a nitrate-limited
567 chemostat, J. Phycol., 50, 243-253, 2014.
568 Heraud, P. and Beardall, J.: Changes in chlorophyll fluorescence during exposure of
569 *Dunaliella tertiolecta* to UV radiation indicate a dynamic interaction between
570 damage and repair processes, Photosynth. Res., 63, 123-134, 2000.
571 Heraud, P., Roberts, S., Shelly, K., and Beardall, J.: Interactions between UV-B
572 exposure and phosphorus nutrition. II. Effects on rates of damage and repair, J.
573 Phycol., 41, 1212-1218, 2005.

574 Hessen, D. O., Leu, E., Færøvig, P. J., and Falk Petersen, S.: Light and spectral
575 properties as determinants of C: N: P-ratios in phytoplankton, Deep-Sea Res.
576 Part II, 55, 2169-2175, 2008.
577 Holm-Hansen, O. and Helbling, E. W.: Técnicas para la medición de la productividad
578 primaria en el fitoplancton. In: Manual de métodos ficológicos, Alveal, K.,
579 Ferrario, M. E., Oliveira, E. C., and Sar, E. (Eds.), Universidad de Concepción,
580 Concepción,Chile, 329-350, 1995.
581 Hopkinson, B. M., Dupont, C. L., Allen, A. E., and Morel, F. M. M.: Efficiency of the
582 CO_2-concentrating mechanism of diatoms, Proc. Natl. Acad. Sci., 108,
583 3830-3837, 2011.
584 Hopkinson, B. M., Xu, Y., Shi, D., McGinn, P. J., and Morel, F. M. M.: The effect of
585 CO_2 on the photosynthetic physiology of phytoplankton in the Gulf of Alaska,
586 Limnol. Oceanogr., 55, 2011-2024, 2010.
587 IPCC: Workshop Report of the Intergovernmental Panel on Climate Change
588 Workshop on Impacts of Ocean Acidification on Marine Biology and
589 Ecosystems. Field, C. B., Barros, V., Stocker, T. F., Qin, D., Mach, K. J., Plattner,
590 G.-K., Mastrandrea, M. D., Tignor, M., and Ebi, K. L. (Eds.), IPCC Working
591 Group II Technical Support Unit, Carnegie Institution, Stanford, California,
592 United States of America, 2011.
593 Kanazawa, A. and Kramer, D. M.: In vivo modulation of nonphotochemical exciton
594 quenching (NPQ) by regulation of the chloroplast ATP synthase, Proc. Natl.
595 Acad. Sci., 99, 12789-12794, 2002.

596 Kim, J. M., Lee, K., Shin, K., Kang, J. H., Lee, H. W., Kim, M., Jang, P. G., and Jang,
597 M. C.: The effect of seawater CO_2 concentration on growth of a natural
598 phytoplankton assemblage in a controlled mesocosm experiment, Limnol.
599 Oceanogr., 51, 1629-1636, 2006.
600 King, A. L., Sañudo-Wilhelmy, S. A., Leblanc, K., Hutchins, D. A., and Fu, F.: CO_2
601 and vitamin B_{12} interactions determine bioactive trace metal requirements of a
602 subarctic Pacific diatom, The ISME journal, 5, 1388-1396, 2011.
603 Leonardos, N. and Geider, R. J.: Elevated atmospheric carbon dioxide increases
604 organic carbon fixation by *Emiliania Huxleyi* (Haptophyta), under
605 nutrient-limited high-light conditions, J. Phycol., 41, 1196-1203, 2005.
606 Lewis, E. and Wallace, D. W. R.: Program developed for CO_2 system calculations. In:
607 ORNL/CDIAC-105, Carbon Dioxide Information Analysis Center, Oak Ridge
608 National Laboratory, US Department of Energy, Oak Ridge, Tennessee, 1998.
609 Li, G., Gao, K., and Gao, G.: Differential impacts of solar UV radiation on
610 photosynthetic carbon fixation from the coastal to offshore surface waters in the
611 South China Sea, Photochem. Photobiol., 87, 329-334, 2011.
612 Li, W., Gao, K., and Beardall, J.: Interactive effects of ocean acidification and
613 nitrogen-limitation on the diatom *Phaeodactylum tricornutum*, PLoS One, 7,
614 e51590, 2012a.
615 Li, Y., Gao, K., Villafañe, V., and Helbling, E.: Ocean acidification mediates
616 photosynthetic response to UV radiation and temperature increase in the diatom
617 *Phaeodactylum tricornutum*, Biogeosciences, 9, 3931-3942, 2012b.

618 Litchman, E., Neale, P. J., and Banaszak, A. T.: Increased sensitivity to ultraviolet
619 radiation in nitrogen-limited dinoflagellates: Photoprotection and repair, Limnol.
620 Oceanogr., 47, 86-94, 2002.
621 Morel, F. M. M., Rueter, J. G., Anderson, D. M., and Guillard, R. R. L.: Aquil: A
622 chemically defined phytoplankton culture medium for trace metal studies, J.
623 Phycol., 15, 135-141, 1979.
624 Neale, P., Sobrino, C., Segovia, M., Mercado, J., Leon, P., Cortés, M., Tuite, P., Picazo,
625 A., Salles, S., and Cabrerizo, M.: Effect of CO_2, nutrients and light on coastal
626 plankton. I. Abiotic conditions and biological responses, Aquat. Biol., 22, 25-41,
627 2014.
628 Nielsen, E. S.: The use of radioactive carbon (C^{14}) for measuring organic production
629 in the sea, Journal du Conseil, 18, 117-140, 1952.
630 Orr, J. C., Fabry, V. J., Aumont, O., Bopp, L., Doney, S. C., Feely, R. A.,
631 Gnanadesikan, A., Gruber, N., Ishida, A., Joos, F., Key, R. M., Lindsay, K.,
632 Maier-Reimer, E., Matear, R., Monfray, P., Mouchet, A., Najjar, R. G., Plattner,
633 G. K., Rodgers, K. B., Sabine, C. L., Sarmiento, J. L., Schlitzer, R., Slater, R. D.,
634 Totterdell, I. J., Weirig, M. F., Yamanaka, Y., and Yool, A.: Anthropogenic ocean
635 acidification over the twenty-first century and its impact on calcifying organisms,
636 Nature, 437, 681-686, 2005.
637 Pörtner, H. O. and Farrell, A. P.: Physiology and climate change, Science, 322,
638 690-692, 2008.
639 Raven, J. A., Giordano, M., Beardall, J., and Maberly, S. C.: Algal and aquatic plant

carbon concentrating mechanisms in relation to environmental change, Photosynth. Res., 109, 281-296, 2011.

Riebesell, U. and Tortell, P. D.: Effects of ocean acidification on pelagic organisms and ecosystems. In: Ocean acidification, Gattuso, J.-P. and Hansson, L. (Eds.), Oxford University Press, New York, 99-121, 2011.

Riebesell, U., Wolf-Gladrow, D. A., and Smetacek, V.: Carbon dioxide limitation of marine phytoplankton growth rates, Nature, 361, 249-251 1993.

Rost, B., Riebesell, U., Burkhardt, S., and Sültemeyer, D.: Carbon acquisition of bloom-forming marine phytoplankton, Limnol. Oceanogr., 48, 55-67, 2003.

Roy, R. N., Roy, L. N., Vogel, K. M., Porter-Moore, C., Pearson, T., Good, C. E., Millero, F. J., and Campbell, D. M.: The dissociation constants of carbonic acid in seawater at salinities 5 to 45 and temperatures 0 to 45 ^{o}C, Mar. Chem., 44, 249-267, 1993.

Shelly, K., Heraud, P., and Beardall, J.: Nitrogen limitation in *Dunaliella tertiolecta* Butcher (Chlorophyceae) leads to increased susceptibility to damage by ultraviolet-B radiation but also increased repair capacity, J. Phycol., 38, 713-720, 2002.

Shi, D., Kranz, S. A., Kim, J. M., and Morel, F. M. M.: Ocean acidification slows nitrogen fixation and growth in the dominant diazotroph *Trichodesmium* under low-iron conditions, Proc. Natl. Acad. Sci., 109, E3094-E3100, 2012.

Sobrino, C., Segovia, M., Neale, P. J., Mercado, J. M., García-Gómez, C., Kulk, G., Lorenzo, M. R., Camarena, T., van de Poll, W. H., Spilling, K., and Ruan, Z.:

Effect of CO_2, nutrients and light on coastal plankton. IV. Physiological responses, Aquat. Biol., 22, 77-93, 2014.

Sobrino, C., Ward, M. L., and Neale, P. J.: Acclimation to elevated carbon dioxide and ultraviolet radiation in the diatom *Thalassiosira pseudonana*: Effects on growth, photosynthesis, and spectral sensitivity of photoinhibition, Limnol. Oceanogr., 53, 494-505, 2008.

Tortell, P. D.: Evolutionary and ecological perspectives on carbon acquisition in phytoplankton, Limnol. Oceanogr., 45, 744-750, 2000.

Wang, M. and Wang, G.: Oxidative damage effects in the copepod *Tigriopus japonicus* Mori experimentally exposed to nickel, Ecotoxicology, 19, 273-284, 2010.

Wu, H. and Gao, K.: Responses of a marine red tide alga *Skeletonema costatum* (Bacillariophyceae) to long-term UV radiation exposures, J. Photoch. Photobio. B, 94, 82-86, 2009.

Wu, H., Gao, K., Villafañe, V. E., Watanabe, T., and Helbling, E. W.: Effects of solar UV radiation on morphology and photosynthesis of filamentous cyanobacterium *Arthrospira platensis*, Appl. Environ. Microb., 71, 5004-5013, 2005.

Wu, Y., Gao, K., and Riebesell, U.: CO_2-induced seawater acidification affects physiological performance of the marine diatom *Phaeodactylum tricornutum*, Biogeosciences, 7, 2915-2923, 2010.

Xu, K. and Gao, K.: Reduced calcification decreases photoprotective capability in the coccolithophorid *Emiliania huxleyi*, Plant Cell Physiol., 53, 1267-1274, 2012.

Zacher, K., Hanelt, D., Wiencke, C., and Wulff, A.: Grazing and UV radiation effects on an Antarctic intertidal microalgal assemblage: a long-term field study, Polar Biol., 30, 1203-1212, 2007.

Zheng, Y. and Gao, K.: Impacts of solar UV radiation on the photosynthesis, growth, and UV-absorbing compounds in *Gracilaria Lemaneiformis* (Rhodophyta) grown at different nitrate concentrations, J. Phycol., 45, 314-323, 2009.

Table 1. Interactive effects among NO_3^- concentrations, CO_2 levels and radiation treatments. Two or three way ANOVA analysis of individual and interactive effects among NO_3^- concentrations, CO_2 levels and radiation treatments. Stars indicate significance at $P < 0.05$. Where "Ni" indicates nitrate, "OA" CO_2/pH, "Rad-Treat" radiation treatments, "Inh-C" inhibition of carbon fixation and "Inh- yield" inhibition of yield.

Parameter	Ni	OA	Rad-Treat	Ni & OA	Ni & Rad-Treat	OA & Rad-Treat	Ni, OA & Rad-Treat
Carbon fixation	*	*	*	*	*		*
Inh-C	*		*		*		*
yield	*		*	*	*		
Inh- yield	*		*	*	*		
NPQ	*		*		*		

Table 2. The PSII damage (k) and repair (r) rate constants (min^{-1}) in *Phaeoductylum tricornutum* cells grown in LC-HN, LC-LN, HC-HN and HC-LN during the 60 min exposures to PAR+ UVA+UVB (44.11 + 14.19 + 0.75 Wm^{-2}). Parameters of repair and damage rates were calculated based on Fig. 2 according to Heraud and Beardall (2000). SD was for triplicate cultures. Treatments with the same lowercase superscript letters, means the difference is not significant. In contrast, treatments with different lowercase superscript letters indicate the difference is significant ($P < 0.05$ level).

	R^2 for fit	Repair rate(r)	Damage rate(k)	r/k
LC-HN	>0.99	0.044 ± 0.007^{a}	0.068 ± 0.007^{a}	0.666 ± 0.216^{ab}
HC-HN	>0.99	0.064 ± 0.019^{ab}	0.079 ± 0.010^{ab}	0.806 ± 0.145^{ab}
LC-LN	>0.99	0.054 ± 0.012^{ab}	0.062 ± 0.008^{a}	0.854 ± 0.138^{a}
HC-LN	>0.99	0.059 ± 0.005^{b}	0.095 ± 0.010^{b}	0.588 ± 0.073^{b}

738 **Table 3.** The exponential rate constant for recovery (R, min^{-1}) under growth light after
739 80 min exposure to solar radiation with or without UV. Different letters of
740 superscripts indicate significant differences between the CO_2 and NO_3^- treatments at P
741 < 0.05.

	LC-HN	LC-LN	HC-HN	HC-LN
P	0.038 ± 0.006^{ab}	0.029 ± 0.011^{b}	0.043 ± 0.009^{a}	0.038 ± 0.002^{ab}
PA	0.028 ± 0.002^{a}	0.023 ± 0.007^{a}	0.037 ± 0.002^{b}	0.027 ± 0.008^{ab}
PAB	0.019 ± 0.002^{a}	0.024 ± 0.001^{b}	0.029 ± 0.003^{c}	0.021 ± 0.003^{d}

742
743
744
745
746
747
748
749
750
751
752
753
754
755

Table 4. The recovery time to half maximal yield values under growth light after 80 min exposure to solar radiation with or without UV. Different letters of superscripts indicate significant differences between the radiation treatments at $P < 0.05$.

	LC-HN (min)	LC-LN (min)	HC-HN (min)	HC-LN (min)
P	16.78 ± 2.94^{a}	20.81 ± 5.93^{a}	15.41 ± 2.57^{ab}	16.79 ± 0.64^{a}
PA	20.38 ± 1.28^{a}	23.36 ± 4.47^{a}	16.83 ± 0.67^{a}	21.66 ± 4.52^{ab}
PAB	25.82 ± 1.51^{b}	22.73 ± 1.25^{a}	20.05 ± 1.78^{b}	24.64 ± 1.57^{b}

Figure captions

Figure 1. Photosynthetic carbon fixation rates of *P. tricornutum* under different treatments. Photosynthetic carbon fixation rates of *P. tricornutum* cells represented as rates (a, b) per cell and (c, d) per chl *a* grown at ambient (390 μatm, LC) or elevated CO_2 (1000 μatm, HC) under NO_3^- replete (110 μmol L^{-1}, HN) (a, c) or limited condition (10 μmol L^{-1}, LN) (b, d) when exposed to PAR (P), PAR+UVA (PA) and PAR+UVA+UVB (PAB) for 60 min, respectively. Vertical bars indicate ±SD, the means and standard deviation were based on 3 replicates. The different lowercase letters indicate significant differences between different treatments at $P < 0.05$ level.

Figure 2. The effective quantum yield of *P. tricornutum* under different treatments. Changes of effective quantum yield in *P. tricornutum* cells at ambient (390 μatm, LC) or elevated CO_2 (1000 μatm, HC) under (a, b) NO_3^- replete (110 μmol L^{-1}, HN) or (c, d) limited (10 μmol L^{-1}, LN) when exposed to PAR (P), PAR+UVA (PA) and PAR+UVA+UVB (PAB) for 60 min and another 80 min under the growth light level (the time of the switch to growth light levels is indicated by the dashed line), respectively. The irradiance intensities under solar simulator or growth light were the same as mentioned above. Vertical bars are means ±SD, n=3.

Figure 3. UV induced inhibition of carbon fixation and PSII activity. UVA and UVB induced inhibition of (a, b) photosynthetic carbon fixation and (c, d) PSII of *P. tricornutum* cells grown at ambient (390 μatm, LC) or elevated CO_2 (1000 μatm, HC)

799 under (a, c) NO_3^- replete (110 μmol L^{-1}, HN) or (b, d) NO_3^- limited condition (10 μmol
800 L^{-1}, LN) when exposed to PAR (P), PAR+UVA (PA) and PAR+UVA+UVB (PAB) for
801 60 min, respectively. The irradiance intensity under solar simulator was the same as
802 mentioned above. Vertical bars are means ±SD, n=3, the different letters indicate
803 significant differences between different treatments at $P < 0.05$ level.
804
805 **Figure 4.** Non-photochemical quenching (NPQ) of *P. tricornutum* under different
806 treatments. NPQ of *P. tricornutum* grown at ambient (390 μatm, LC) or elevated CO_2
807 (1000 μatm, HC) under (a, b) NO_3^- replete (110 μmol L^{-1}, HN) or (c, d) limited
808 condition (10 μmol L^{-1}, LN) when exposed to PAR (P), PAR+UVA (PA) and
809 PAR+UVA+UVB (PAB) for 60 min and another 80 min under the growth light level,
810 respectively. The irradiance intensities under solar simulator or growth light were the
811 same as mentioned above. Vertical bars means ±SD, n=3.
812
813 **Figure 5.** Protein contents, SOD and CAT activities of *P. tricornutum* under different
814 treatments. (a) Protein contents, (b) SOD and (c) CAT activities (represented as per
815 milligram protein) of *P. tricornutum* grown at ambient (390 μatm, LC) or elevated
816 CO_2 (1000 μatm, HC) under NO_3^- replete (110 μmol L^{-1}, HN) or limited (10 μmol L^{-1},
817 LN). The different letters above each column indicate significant differences between
818 different treatments at $P < 0.05$ level. Vertical bars means ±SD, except the CAT value
819 in HC-LN for which there were only 2 replicates, other treatments used at least 3
820 replicates (n=3-7).

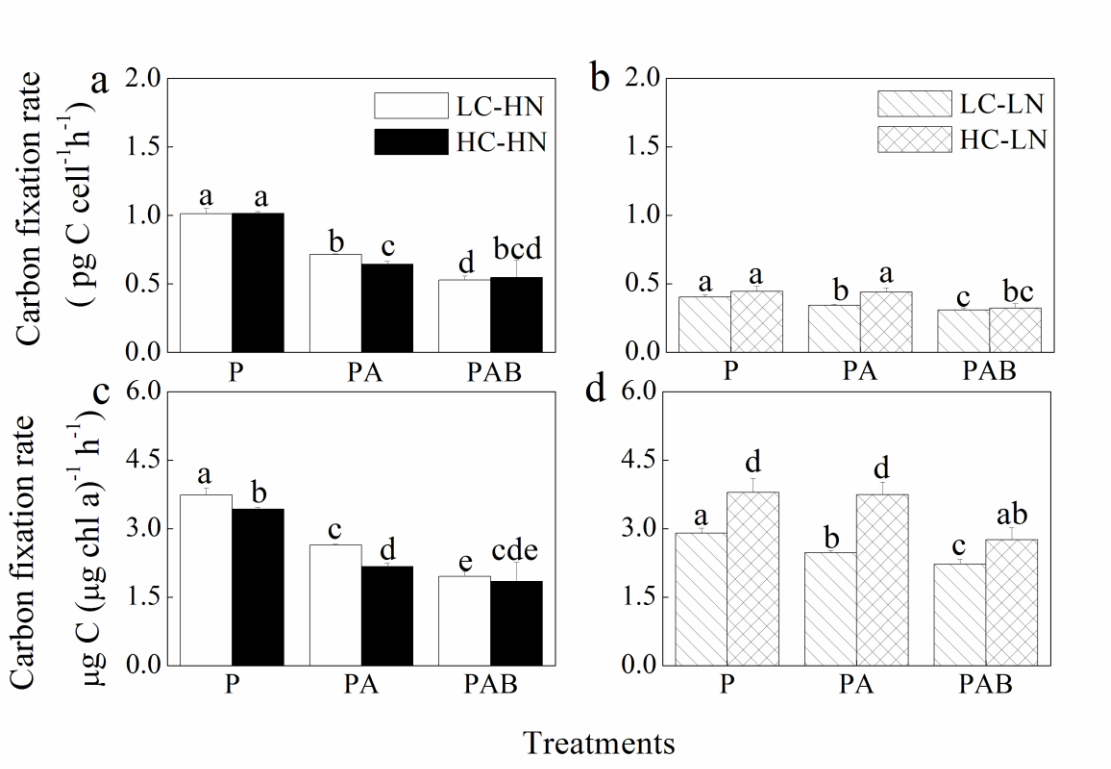
a
b
c
d
LC-HN
HC-HN
LC-LN
HC-LN
Carbon fixation rate
(pg C cell-1h-1)
Carbon fixation rate
μg C (μg chl a)-1 h-1)
P
PA
PAB
Treatments

Fig. 1

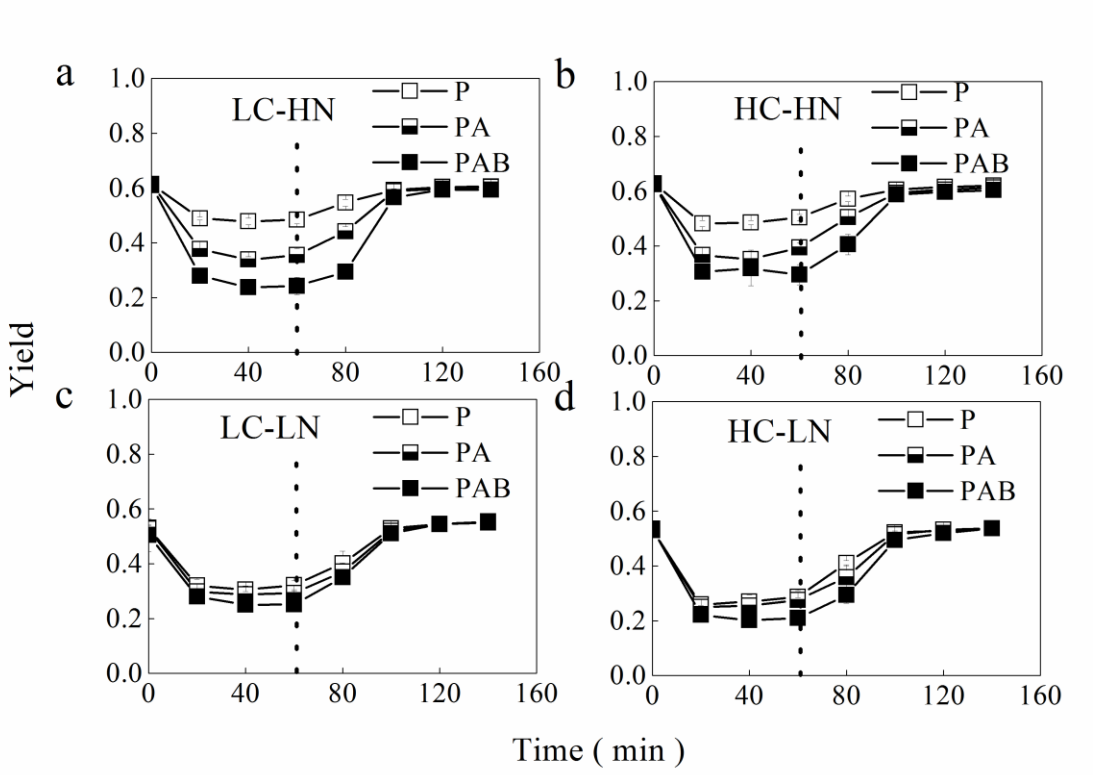
a
LC-HN
P
PA
PAB
b
HC-HN
c
LC-LN
d
HC-LN
Yield
Time (min)
0.0
0.2
0.4
0.6
0.8
1.0
0
40
80
120
160

Fig. 2

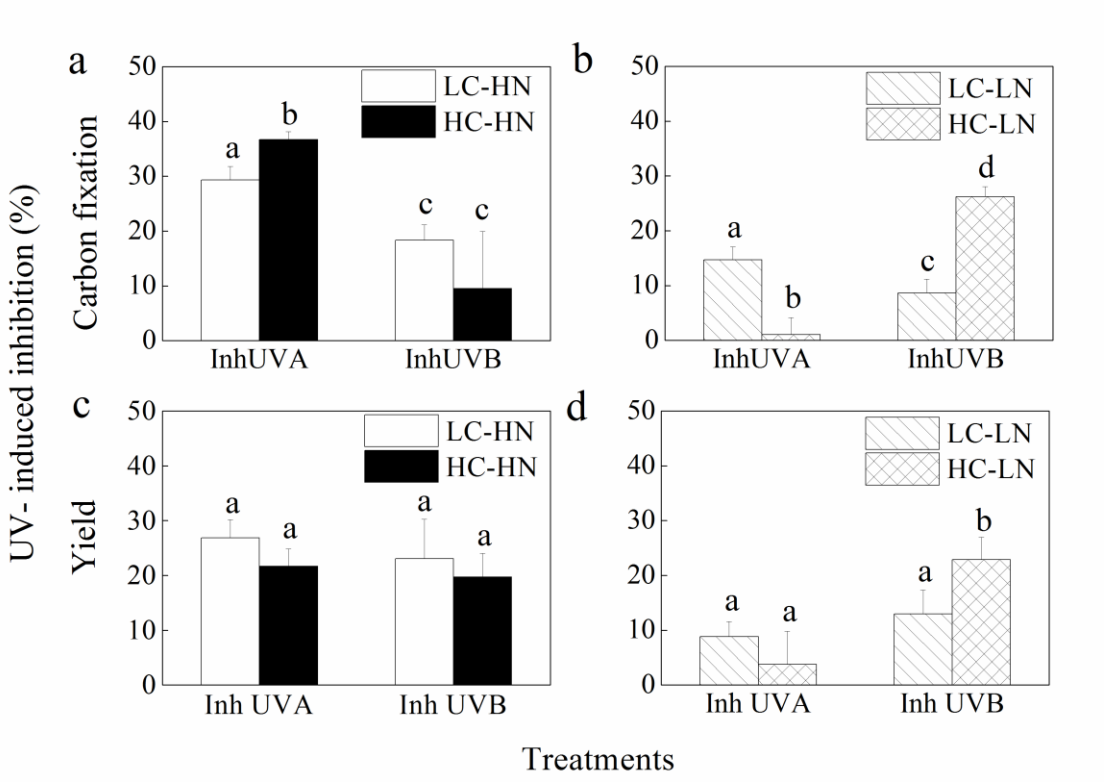
a
Carbon fixation
LC-HN
HC-HN
InhUVA
InhUVB
b
LC-LN
HC-LN
c
Yield
Inh UVA
Inh UVB
d
UV- induced inhibition (%)
Treatments

Fig. 3

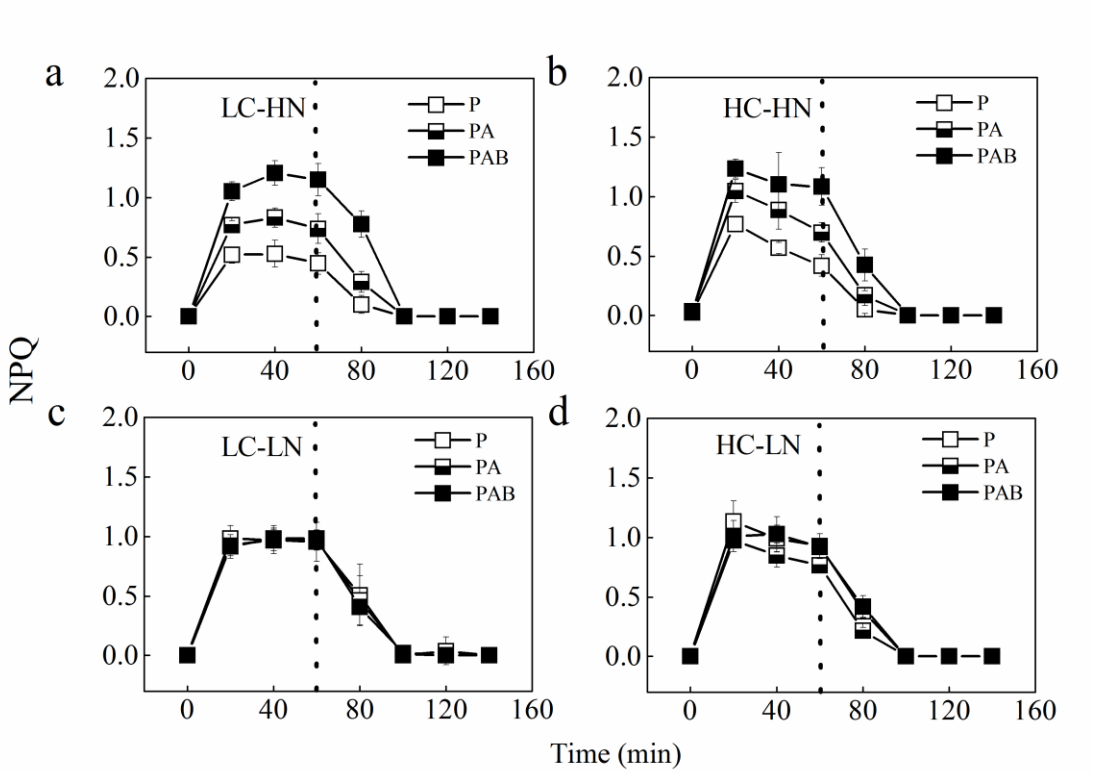
a
LC-HN
b
HC-HN
c
LC-LN
d
HC-LN
P
PA
PAB
NPQ
Time (min)
0.0
0.5
1.0
1.5
2.0
0
40
80
120
160

Fig. 4

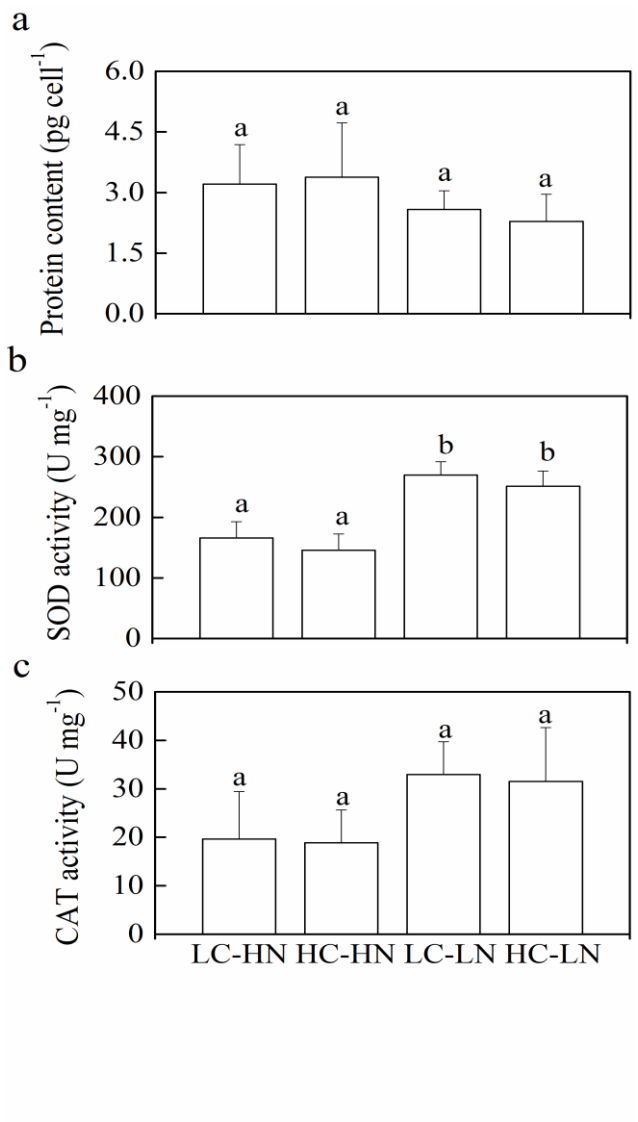

877

878 Fig. 5

879